

Manipulation of helical states revealed by crossed Andreev reflection

Wei Luo^{1,2}, Yating Zhang¹, and Wei Chen^{1*}

¹ National Laboratory of Solid State Microstructures,

School of Physics, Jiangsu Physical Science Research Center,

and Collaborative Innovation Center of Advanced Microstructures, Nanjing University, Nanjing 210093, China

² School of Science, Jiangxi University of Science and Technology, Ganzhou 341000, China

(Dated: November 27, 2024)

The edge states of a quantum spin Hall insulator exhibit helical properties, which has generated significant interest in the field of spintronics. Although it is predicted theoretically that Rashba spin-orbit coupling can effectively regulate edge state spin, experimental characterization of this spin control remains challenging. Here, we propose utilizing crossed Andreev reflection to probe the efficiency of gate voltage control on edge state spin. We calculate the transport properties of the quantum spin Hall isolators-superconductor heterojunction by using non-equilibrium Green's function method. We find that the probabilities of crossed Andreev reflection, electron transmission, and non-local conductance all include the relative spin rotation angle θ caused by the Rashba spin-orbit coupling in the helical edge states. Notably, when the incident energy is close to the superconducting gap, the differential conductance $G_2 \propto -\cos\theta$. Thus, the influence of Rashba spin-orbit coupling on edge state spin can be quantitatively characterized by crossed Andreev reflection, which provides a feasible scheme for experimental testing.

I. INTRODUCTION

Quantum spin Hall insulator (QSHI) is a topologically nontrivial phase of electronic matter, which has a bulk insulating gap with gapless edge states traversing this gap [1–6]. These edge states are protected from impurity scattering by the nontrivial bulk band topology and time reversal symmetry. Due to the spin-momentum locking [7, 8] in the edge states, QSHIs have garnered significant interest in the field of spintronics [9–12]. Compared to traditional electronics, spintronics offers several advantages, including higher information density, lower power consumption, and the potential for novel electronic devices and technologies [13, 14]. Consequently, spintronics holds extensive application prospects in areas such as information storage [15], quantum computing [16], and sensing devices [17].

A fundamental aspect of spintronics is spin control, which entails the precise manipulation of spin direction and its dynamic evolution through external fields for applications in information storage and processing. In QSHIs, spin-momentum locking manifests as a consequence of spin-orbit coupling (SOC) in the edge states, indicating that the electron spin can be influenced by external fields that affect the spatial wave function. By imposing a perpendicular electric field E_z , the Rashba spin-orbit coupling can be generated [18–20], which provides a convenient and efficient method for manipulating edge state spin [21–25]. The control of Rashba SOC through gate voltage is a central topic in semiconductor spintronics [26], benefiting from relatively mature technology that facilitates its integration into QSHIs. Although theoretical predictions suggest that Rashba SOC can effectively regulate edge state spin, experimental characterization of

this spin control remains challenging due to its subtlety in conventional transport measurements. Therefore, it is crucial to develop a viable and quantifiable approach to assess the efficiency of Rashba SOC in controlling edge state spin.

In this work, we propose utilizing crossed Andreev reflection (CAR) [27, 28] to probe the efficiency of gate voltage in regulating edge state spin. The proposed setup is shown in Fig. 1, two QSHIs close to each other are in contact with an s -wave superconductor (SC). Coherent reflection between the QSHIs can occur if they are sufficiently close, e.g., on the order of the coherence length ξ of the SC. s -wave SCs require the pairing of electrons with opposite spins. Consequently, when an electron with spin \mathbf{m} is incident, it attracts an electron with spin $-\mathbf{m}$ into the SC, leaving behind a reflected hole with spin \mathbf{m} . In the absence of Rashba SOC, adjacent edge states exhibit opposite helicities, as shown in Fig. 1(a). Such spin configurations prevent an incoming spin-up electron at edge 1 from pairing with a spin-down outgoing electron that is absent at edge 2, thus inhibiting CAR. However, Rashba SOC exerts a uniform effect on the spins of both sets of edge states, unlike helicity, which possesses opposite values for different edges. As a result, the spin polarization directions of adjacent edge states rotate in opposite directions, as illustrated in Fig. 1(b). Under Rashba SOC, the spin of the incident electron at edge 1 rotates clockwise towards the \mathbf{m} direction, while the spin of the outgoing electron at edge 2 rotates counterclockwise towards the $-\mathbf{n}$ direction. Since the s -wave SC pairs electrons with opposite spins, the CAR amplitude is expected to be proportional to $\langle -\mathbf{m} | -\mathbf{n} \rangle$, with $|-\mathbf{m}\rangle (|-\mathbf{n}\rangle)$ representing the spin state polarized along the $-\mathbf{m}$ ($-\mathbf{n}$) direction, which is related to the strength of the Rashba SOC. In this way, CAR can be used to quantitatively characterize the effect of Rashba SOC on edge state spin, thereby providing a viable approach for

* pchenweis@gmail.com

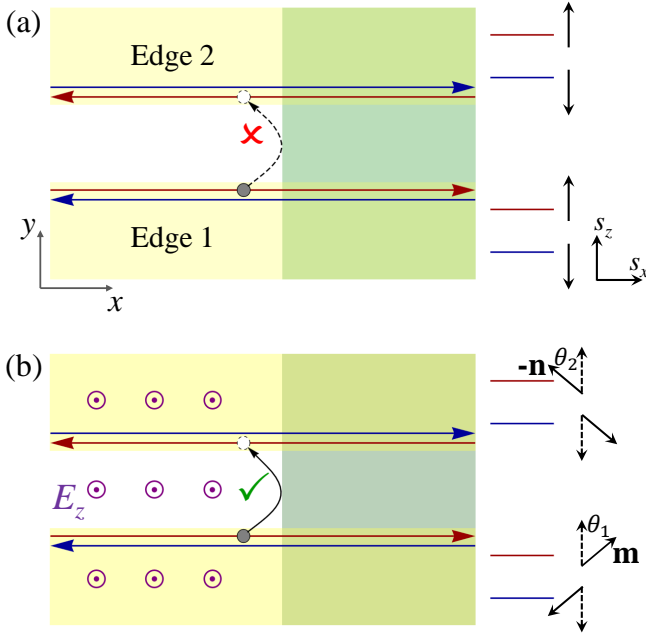


FIG. 1. (Color online) Schematic illustration of the proposed structure. Two QSHIs in close proximity are in contact with the s -wave SC. In (a), where there is no Rashba SOC, the opposite helicities of the adjacent edge states prevent CAR. In (b), a perpendicular electric field E_z induces Rashba SOC, causing the spin rotation directions of adjacent edge states to be opposite. The spin of the incoming electrons at edge 1 rotates clockwise, while the spin of the outgoing state at edge 2 rotates counterclockwise. As a result, the incoming state and the outgoing hole are no longer orthogonal, allowing CAR to occur.

experimental verification.

The rest of the paper is organized as follows. In Sec. II we present the model and derive the transport coefficients and current. The numerical results are discussed in Sec. III, and finally, we draw our conclusions in Sec. IV.

II. MODEL

In the following, we calculate the transport properties of the QSHIs-SC heterojunction using non-equilibrium Green's function method to obtain rigorous results. The Hamiltonian for the helical edge states is given by

$$H_E = \sum_{\alpha p} s_{\alpha} v p (c_{\alpha p \uparrow}^{\dagger} c_{\alpha p \uparrow} - c_{\alpha p \downarrow}^{\dagger} c_{\alpha p \downarrow}), \quad (1)$$

where $c_{\alpha p \uparrow(\downarrow)}$ are the annihilation operators for electrons with spin $\uparrow(\downarrow)$ and momentum p , and v is the Fermi velocity. The edge index $\alpha = 1, 2$, and $s_1 = 1, s_2 = -1$ capture the spin helicities of the edge states. To manipulate the spins of the edge states, we apply a perpendicular electric field E_z to the QSHIs, which induces Rashba

SOC described by

$$H_R = \lambda_{\alpha} p (c_{\alpha p \uparrow}^{\dagger} c_{\alpha p \downarrow} + c_{\alpha p \downarrow}^{\dagger} c_{\alpha p \uparrow}), \quad (2)$$

where the Rashba coefficient satisfies $\lambda_{\alpha} \propto e E_z$. The Rashba SOC is equivalent to a nonuniform Zeeman field, which changes the spin directions of the helical edge states. Let us first examine edge 1. By combining Eqs. (1) and (2), one obtains the eigenvalues $\varepsilon_{1\pm} = \pm v_1 p$, where $v_1 = \sqrt{v^2 + \lambda_1^2}$. The corresponding eigenstates are given by

$$|\mathbf{m}\rangle = \cos \frac{\theta_1}{2} |\uparrow\rangle + \sin \frac{\theta_1}{2} |\downarrow\rangle, \\ |-\mathbf{m}\rangle = -\sin \frac{\theta_1}{2} |\uparrow\rangle + \cos \frac{\theta_1}{2} |\downarrow\rangle,$$

with $\theta_1 = \arctan(\lambda_1/v)$. The electrons in states $|\mathbf{m}\rangle$ have spins parallel to the direction $\mathbf{m} = \langle \mathbf{m} | \boldsymbol{\sigma} | \mathbf{m} \rangle = (\sin \theta_1, 0, \cos \theta_1)$, while the electrons in $|-\mathbf{m}\rangle$ have opposite spins. The Rashba SOC induces a clockwise rotation of the spins of edge states by an angle θ_1 , as illustrated in Fig. 1(b). For edge 2, the eigenvalues are $\varepsilon_{2\pm} = \pm v_2 p$, where $v_2 = \sqrt{v^2 + \lambda_2^2}$. The corresponding eigenstates are

$$|\mathbf{n}\rangle = \sin \frac{\theta_2}{2} |\uparrow\rangle + \cos \frac{\theta_2}{2} |\downarrow\rangle, \\ |-\mathbf{n}\rangle = \cos \frac{\theta_2}{2} |\uparrow\rangle - \sin \frac{\theta_2}{2} |\downarrow\rangle,$$

with spins pointing to $\mathbf{n} = (\sin \theta_2, 0, \cos \theta_2)$ and $-\mathbf{n}$, respectively, where $\theta_2 = \arctan(\lambda_2/v)$. For edge 2, Rashba SOC causes a counterclockwise rotation of the spin by an angle θ_2 , as shown Fig. 1(b).

The SC is described by the following Hamiltonian

$$H_S = \sum_{k\sigma} \varepsilon_k d_{k\sigma}^{\dagger} d_{k\sigma} + \Delta \sum_k (d_{k\uparrow}^{\dagger} d_{-k\downarrow}^{\dagger} + d_{-k\downarrow} d_{k\uparrow}), \quad (3)$$

where $d_{k\sigma}$ are the annihilation operators for electrons with momentum k and spin $\sigma = \uparrow, \downarrow$, and Δ is the pair potential. The coupling between QSHIs and SC is

$$H_T = \sum_{\alpha p k \sigma} (T_{\alpha p k} c_{\alpha p \sigma}^{\dagger} d_{k\sigma} + T_{k \alpha p} d_{k\sigma}^{\dagger} c_{\alpha k \sigma}), \quad (4)$$

with $T_{\alpha k p}$ the tunneling strength, satisfying $T_{\alpha k p} = T_{p \alpha k}^*$.

It is convenient to calculate the transport properties using the spin eigenstate representations of edges 1 and 2. The corresponding bases are $(c_{1p m}, c_{1p \bar{m}})$ and $(c_{2p n}, c_{2p \bar{n}})$, with subscripts m (\bar{m}) representing states $|\mathbf{m}\rangle$ ($|-\mathbf{m}\rangle$), and n (\bar{n}) representing $|\mathbf{n}\rangle$ ($|-\mathbf{n}\rangle$). Additionally, the scattering region includes the SC, so we will work in the Nambu space. The Hamiltonian of the helical edge states is then expressed as

$$\mathcal{H}_E = \sum_p (\tilde{c}_{1p}^{\dagger} h_{1p} \tilde{c}_{1p} + \tilde{c}_{2p}^{\dagger} h_{2p} \tilde{c}_{2p}), \\ h_{\alpha p} = \begin{pmatrix} v_{\alpha} p & 0 & 0 & 0 \\ 0 & -v_{\alpha} p & 0 & 0 \\ 0 & 0 & v_{\alpha} p & 0 \\ 0 & 0 & 0 & -v_{\alpha} p \end{pmatrix}, \quad (5)$$

with Nambu bases $\tilde{c}_{1p} = (c_{1pm}, c_{1p\bar{m}}, c_{1\bar{p}m}^\dagger, c_{1\bar{p}\bar{m}}^\dagger)^T$ and $\tilde{c}_{2p} = (c_{2pn}, c_{2p\bar{n}}, c_{2\bar{p}n}^\dagger, c_{2\bar{p}\bar{n}}^\dagger)^T$. For simplicity, we express the superconducting Hamiltonian in the spin basis $|\pm \mathbf{m}\rangle$ as well

$$\mathcal{H}_S = \sum_k \tilde{d}_k^\dagger h_S \tilde{d}_k, \quad (6)$$

$$h_S = \begin{pmatrix} \varepsilon_k & 0 & 0 & \Delta \\ 0 & \varepsilon_k & -\Delta & 0 \\ 0 & -\Delta & -\varepsilon_{-k} & 0 \\ \Delta & 0 & 0 & -\varepsilon_{-k} \end{pmatrix},$$

with $\tilde{d}_k = (d_{km}, d_{k\bar{m}}, d_{k\bar{m}}^\dagger, d_{km}^\dagger)^T$. The coupling Hamiltonian is given by

$$\mathcal{H}_T = \sum_{pk} (\tilde{c}_{1p}^\dagger t_{1pk} \tilde{d}_k + \tilde{c}_{2p}^\dagger t_{2pk} \tilde{d}_k + \text{H.c.}), \quad (7)$$

where the hopping matrices t_{1pk} and t_{2pk} are defined as

$$t_{1pk} = \begin{pmatrix} T_{1pk} & 0 & 0 & 0 \\ 0 & T_{1pk} & 0 & 0 \\ 0 & 0 & -T_{1\bar{p}\bar{k}}^* & 0 \\ 0 & 0 & 0 & -T_{1\bar{p}\bar{k}}^* \end{pmatrix},$$

and

$$t_{2pk} = \begin{pmatrix} T_{2pk}^{nm} & T_{2pk}^{n\bar{m}} & 0 & 0 \\ T_{2pk}^{n\bar{m}} & T_{2pk}^{nm} & 0 & 0 \\ 0 & 0 & -T_{2\bar{p}\bar{k}}^{nm*} & -T_{2\bar{p}\bar{k}}^{n\bar{m}*} \\ 0 & 0 & -T_{2\bar{p}\bar{k}}^{n\bar{m}*} & -T_{2\bar{p}\bar{k}}^{nm*} \end{pmatrix},$$

with $T_{2pk}^{nm} = \sin(\theta/2)T_{2pk}$, $T_{2pk}^{n\bar{m}} = \cos(\theta/2)T_{2pk}$, $T_{2pk}^{n\bar{m}} = \cos(\theta/2)T_{2pk}$, $T_{2pk}^{nm} = -\sin(\theta/2)T_{2pk}$, and $\theta = \theta_1 + \theta_2$.

We focus on the current in the edge 2 which is given by

$$I_2(t) = -e \langle \dot{N}_2(t) \rangle = \frac{ie}{\hbar} \langle [N_2, H] \rangle \quad (8)$$

$$= \frac{2e}{\hbar} \text{Re} \left\{ \sum_{pk} \text{Tr} [\tau_z t_{2pk} \mathbf{G}_{k2p}^<(t, t)] \right\},$$

where the Green's function $\mathbf{G}_{k2p}^<(t, t)$ is defined as $\mathbf{G}_{k2p}^<(t, t') = i \langle [\tilde{c}_{2p}^\dagger(t')]^T [\tilde{d}_k(t)]^T \rangle$.

Performing analytic continuation, the Green's function can be written as

$$\mathbf{G}_{k2p}^<(t, t') = \sum_{k'} \int dt_1 \left[\mathbf{G}_{kk'}^R(t, t_1) t_{2pk'}^\dagger(t_1) \mathbf{g}_{2p}^<(t_1, t') \right. \\ \left. + \mathbf{G}_{kk'}^<(t, t_1) t_{2pk'}^\dagger(t_1) \mathbf{g}_{2p}^A(t_1, t') \right], \quad (9)$$

here, $\mathbf{G}_{kk'}^<(t, t') = i \langle [\tilde{d}_k^\dagger(t')]^T [\tilde{d}_{k'}(t)]^T \rangle$ and $\mathbf{G}_{kk'}^R(t, t') = -i \Theta(t-t') \langle \{ \tilde{d}_k(t) \tilde{d}_{k'}^\dagger(t') + [\tilde{d}_{k'}^\dagger(t')]^T [\tilde{d}_k(t)]^T \} \rangle$ are the lesser and retarded Green's functions of SC, and $\mathbf{g}_{2p}^A(t, t')$ is the bare Green's function in the edge 2 which

is diagonal in Nambu space. The bare Green's functions in edge α are given by

$$\mathbf{g}_{\alpha p}^<(t, t') = i \langle (\tilde{c}_{\alpha p}^\dagger)^T (\tilde{c}_{\alpha p})^T \rangle^T \\ = \text{Diag} [i f_\alpha(\epsilon_\alpha^{p\sigma}) e^{-i\epsilon_\alpha^{p\sigma}(t-t')}, i f_\alpha(\epsilon_\alpha^{p\bar{\sigma}}) e^{-i\epsilon_\alpha^{p\bar{\sigma}}(t-t')}, \\ i [1 - f_\alpha(\epsilon_\alpha^{\bar{p}\sigma})] e^{i\epsilon_\alpha^{\bar{p}\sigma}(t-t')}, i [1 - f_\alpha(\epsilon_\alpha^{\bar{p}\bar{\sigma}})] e^{i\epsilon_\alpha^{\bar{p}\bar{\sigma}}(t-t')}], \\ \mathbf{g}_{\alpha p}^{r,a}(t, t') = \mp i \Theta(\pm t \mp t') \langle [\tilde{c}_{\alpha p} \tilde{c}_{\alpha p}^\dagger + (\tilde{c}_{\alpha p}^\dagger)^T (\tilde{c}_{\alpha p})^T] \rangle^T \\ = \mp i \Theta(\pm t \mp t') \times \text{Diag} [e^{-i\epsilon_\alpha^{p\sigma}(t-t')}, \\ e^{-i\epsilon_\alpha^{p\bar{\sigma}}(t-t')}, e^{i\epsilon_\alpha^{\bar{p}\sigma}(t-t')}, e^{i\epsilon_\alpha^{\bar{p}\bar{\sigma}}(t-t')}], \quad (10)$$

where $\epsilon_\alpha^{p\sigma}$ is the energy of an electron in edge α with momentum p and spin σ with $\sigma = \mathbf{m}(\mathbf{n})$ for $\alpha = 1(2)$, and $f_\alpha(\epsilon)$ is the Fermi-Dirac distribution function. Substituting Eqs. (9) and (10) into Eq. (8), one can derive the current

$$I_2 = \frac{ie}{\hbar} \sum_{kk'} \int \frac{d\epsilon}{2\pi} \text{Tr} \left\{ \tau_z \mathbf{\Gamma}_2^{k'k} \mathbf{G}_{kk'}^<(\epsilon) \right. \\ \left. + \tau_z \mathbf{\Gamma}_2^{k'k} \mathbf{f}_2(\epsilon) [\mathbf{G}_{kk'}^r(\epsilon) - \mathbf{G}_{kk'}^a(\epsilon)] \right\}, \quad (11)$$

where $\mathbf{\Gamma}_2^{k'k} = 2\pi t_{k'2p} \rho_2(\epsilon) t_{2pk}$ is the linewidth function, and $\rho_2(\epsilon) = \text{Diag} [\rho_{2n}^e(\epsilon), \rho_{2\bar{n}}^e(\epsilon), \rho_{2n}^h(\epsilon), \rho_{2\bar{n}}^h(\epsilon)]$, with $\rho_{2n}^e(\bar{n})(\epsilon)$ and $\rho_{2n}^h(\bar{n})(\epsilon) = \rho_{2n}^e(\bar{n})(-\epsilon)$ being the electron and hole densities of states, respectively. In the presence of time reversal symmetry, the density of states is the same for different spins $\rho_{2n} = \rho_{2\bar{n}}$. Therefore, the linewidth function is diagonal $\mathbf{\Gamma}_2^{k'k} = \text{Diag} [\Gamma_{2e}^{k'km}, \Gamma_{2e}^{k'k\bar{m}}, \Gamma_{2h}^{k'km}, \Gamma_{2h}^{k'k\bar{m}}]$, with $\Gamma_{2e}^{k'km} = 2\pi T_{k'2p} T_{2pk} [\rho_{2n}^e \sin^2(\theta/2) + \rho_{2\bar{n}}^e \cos^2(\theta/2)]$, $\Gamma_{2e}^{k'k\bar{m}} = 2\pi T_{k'2p} T_{2pk} [\rho_{2n}^e \cos^2(\theta/2) + \rho_{2\bar{n}}^e \sin^2(\theta/2)]$, $\Gamma_{2h}^{k'km} = 2\pi T_{k'2\bar{p}} T_{2\bar{p}k} [\rho_{2n}^h \sin^2(\theta/2) + \rho_{2\bar{n}}^h \cos^2(\theta/2)]$, and $\Gamma_{2h}^{k'k\bar{m}} = 2\pi T_{k'2\bar{p}} T_{2\bar{p}k} [\rho_{2n}^h \cos^2(\theta/2) + \rho_{2\bar{n}}^h \sin^2(\theta/2)]$. In the following calculations, we assume that the tunneling strength is independent of p and k , and denote the line width function as $\mathbf{\Gamma}_2^{k'k} = \Gamma_2$. $\mathbf{f}_2(\epsilon) = \text{Diag} [f_2^e(\epsilon), f_2^e(\epsilon), f_2^h(\epsilon), f_2^h(\epsilon)]$ is the distribution function matrix with $f_2^e(\epsilon) = f_2(\epsilon)$ and $f_2^h(\epsilon) = 1 - f_2(-\epsilon)$.

The lesser Green's function can be solved by the Keldysh equation

$$\mathbf{G}_{kk'}^<(\epsilon) = \sum_{k_1 k_2} \mathbf{G}_{kk_1}^r \Sigma_{k_1 k_2}^< \mathbf{G}_{k_2 k'}^a, \quad (12)$$

where the self-energy $\Sigma_{k_1 k_2}^<(\epsilon) = \sum_{\alpha p} t_{k_1 \alpha p} \mathbf{g}_{\alpha p}^<(\epsilon) t_{\alpha p k_2}$ is due to the coupling with the two edges. Using Eq. (10), we have

$$\mathbf{g}_{\alpha p}^<(\epsilon) = \int dt e^{i\epsilon t} \mathbf{g}_{\alpha p}^<(t) \\ = 2\pi i \times \text{Diag} [f_\alpha(\epsilon_\alpha^{p\sigma}) \delta(\epsilon - \epsilon_\alpha^{p\sigma}), f_\alpha(\epsilon_\alpha^{p\bar{\sigma}}) \delta(\epsilon - \epsilon_\alpha^{p\bar{\sigma}}), \\ [1 - f_\alpha(\epsilon_\alpha^{\bar{p}\sigma})] \delta(\epsilon + \epsilon_\alpha^{\bar{p}\sigma}), [1 - f_\alpha(\epsilon_\alpha^{\bar{p}\bar{\sigma}})] \delta(\epsilon + \epsilon_\alpha^{\bar{p}\bar{\sigma}})], \quad (13)$$

$$\begin{aligned} \mathbf{g}_{\alpha p}^{r,a}(\epsilon) &= \int dt e^{i\epsilon t} \mathbf{g}_{\alpha p}^{r,a}(t) \\ &= \text{Diag}[(\epsilon - \epsilon_{\alpha}^{p\sigma} \pm i0^+)^{-1}, (\epsilon - \epsilon_{\alpha}^{p\bar{\sigma}} \pm i0^+)^{-1}, \\ &\quad (\epsilon + \epsilon_{\alpha}^{p\sigma} \pm i0^+)^{-1}, (\epsilon + \epsilon_{\alpha}^{p\bar{\sigma}} \pm i0^+)^{-1}], \end{aligned} \quad (14)$$

which yield self-energy

$$\Sigma_{kk'}^< = i \left[\Gamma_1^{kk'} \mathbf{f}_1 + \Gamma_2^{kk'} \mathbf{f}_2 \right], \Sigma_{kk'}^{r,a} = \mp \frac{i}{2} \left[\Gamma_1^{kk'} + \Gamma_2^{kk'} \right], \quad (15)$$

with $\Gamma_1^{k'k} = 2\pi t_{k'1p} \rho_1(\epsilon) t_{1pk}$. Applying the Dyson equation $(\mathbf{G}_{kk'}^{r,a})^{-1} = (\mathbf{g}_k^{r,a})^{-1} - \Sigma_{kk'}^{r,a}$ with $\mathbf{g}_k^{r,a}$ the bare Green's function, one can obtain

$$\mathbf{G}_{kk'}^r - \mathbf{G}_{kk'}^a = \sum_{k_1 k_2} \mathbf{G}_{kk_1}^r [\Sigma_{k_1 k_2}^r - \Sigma_{k_1 k_2}^a] \mathbf{G}_{k_2 k'}^a. \quad (16)$$

Inserting Eqs. (12) and (16) into Eq. (11) yields

$$\begin{aligned} I_2 &= \frac{e}{\hbar} \int d\epsilon \text{Tr} \{ (f_2^e - f_1^e) \Gamma_2^{ee} \mathbf{G}_{ee}^r \Gamma_1^{ee} \mathbf{G}_{ee}^a + (f_2^e - f_1^h) \Gamma_2^{ee} \mathbf{G}_{eh}^r \Gamma_1^{hh} \mathbf{G}_{he}^a + (f_2^e - f_2^h) \Gamma_2^{ee} \mathbf{G}_{eh}^r \Gamma_2^{hh} \mathbf{G}_{he}^a \\ &\quad - (f_2^h - f_1^h) \Gamma_2^{hh} \mathbf{G}_{he}^r \Gamma_1^{ee} \mathbf{G}_{eh}^a - (f_2^h - f_1^h) \Gamma_2^{hh} \mathbf{G}_{hh}^r \Gamma_1^{hh} \mathbf{G}_{hh}^a - (f_2^h - f_2^e) \Gamma_2^{hh} \mathbf{G}_{he}^r \Gamma_1^{ee} \mathbf{G}_{eh}^a \}, \end{aligned} \quad (17)$$

Assuming a bias voltage eV is applied to the edge 1, the edge 2 and the SC are grounded. Thus at low temperature limit, we only need to consider the case of electrons incident from edge 1. Since the edge states are helical, the incident state can only be the spin state $|\mathbf{m}\rangle$. Then we can derive the coefficients of electron transmission and CAR processes

$$\begin{aligned} T_N(\epsilon) &= \text{Tr}[\Gamma_2^{ee} \mathbf{G}_{ee}^r \Gamma_1^{ee} \mathbf{G}_{ee}^a] \\ &= \Gamma_1 \Gamma_2 \sum_{kk_1 k_2 k'} \sum_{\sigma_1 \sigma_2} [G_{kk_1 \sigma_2 m}^{r ee} G_{k_2 k' m \sigma_1}^{a ee}], \end{aligned} \quad (18)$$

$$T_{\text{CAR}}(\epsilon) = \Gamma_1 \Gamma_2 \sum_{kk_1 k_2 k'} \sum_{\sigma_1 \sigma_2} [G_{kk_1 \sigma_2 m}^{r he} G_{k_2 k' m \sigma_1}^{a eh}]. \quad (19)$$

In what follows we calculate the full Green's function in the SC taking into account the coupling effect. The full Green's function in the SC is

$$\mathbf{G}_{kk'}^r(\epsilon) = \mathbf{g}_k^r(\epsilon) \delta_{kk'} + \mathbf{g}_k^r(\epsilon) \Sigma^r(\epsilon) \sum_{k_1} \mathbf{G}_{k_1 k'}^r(\epsilon), \quad (20)$$

where the self-energy subscripts k and k' are omitted, and the bare Green's function $\mathbf{g}_k^r(\epsilon)$ is given by

$$\begin{aligned} \mathbf{g}_k^r(\epsilon) &= [\epsilon + i0^+ - \mathcal{H}_S]^{-1} \\ &= \frac{\epsilon + i0^+ + \epsilon_k \tau_z - \Delta \tau_y \sigma_y}{(\epsilon + i0^+)^2 - \epsilon_k^2 - \Delta^2}. \end{aligned} \quad (21)$$

In order to solve the self-consistent Eq. (20), we denote the summation as

$$\Lambda_{k'}^r(\epsilon) = \sum_{k_1} \mathbf{G}_{k_1 k'}^r(\epsilon),$$

then the Eq. (20) reduces to

$$\mathbf{G}_{kk'}^r(\epsilon) = \mathbf{g}_k^r(\epsilon) \delta_{kk'} + \mathbf{g}_k^r(\epsilon) \Sigma^r(\epsilon) \Lambda_{k'}^r(\epsilon). \quad (22)$$

Sum over k both sides $\Lambda_{k'}^r(\epsilon) = \mathbf{g}_{k'}^r(\epsilon) + \left[\sum_k \mathbf{g}_k^r(\epsilon) \right] \Sigma^r(\epsilon) \Lambda_{k'}^r(\epsilon)$, we can obtain

$$\Lambda_{k'}^r(\epsilon) = \frac{1}{1 - \left[\sum_k \mathbf{g}_k^r(\epsilon) \right] \Sigma^r(\epsilon)} \mathbf{g}_{k'}^r(\epsilon). \quad (23)$$

By summing up both sides of Eq. (22) over k and k' , one can obtain

$$\begin{aligned} \sum_{kk'} \mathbf{G}_{kk'}^r(\epsilon) &= \sum_k \mathbf{g}_k^r(\epsilon) + \left[\sum_k \mathbf{g}_k^r(\epsilon) \right] \Sigma^r(\epsilon) \\ &\quad \times \frac{1}{1 - \left[\sum_k \mathbf{g}_k^r(\epsilon) \right] \Sigma^r(\epsilon)} \left[\sum_{k'} \mathbf{g}_{k'}^r(\epsilon) \right]. \end{aligned} \quad (24)$$

The sum of the bare Green's function $\mathbf{g}_k^r(\epsilon)$ over k is

$$\begin{aligned} \sum_k \mathbf{g}_k^r(\epsilon) &= \int d\epsilon_k \rho_S(\epsilon_k) \mathbf{g}_k^r(\epsilon) \\ &= -i\pi \rho_S^0 \frac{\epsilon - \Delta \tau_y \sigma_y}{\sqrt{\epsilon^2 - \Delta^2}} = -i\pi \rho_S \left(1 - \frac{\Delta}{\epsilon} \tau_y \sigma_y \right). \end{aligned} \quad (25)$$

where ρ_S is the density of the states of the quasi-particle in the SC, and ρ_S^0 is the normal metallic state density. Substituting Eq. (25) into Eq. (24) yields

$$\sum_{kk'} \mathbf{G}_{kk'}^r(\epsilon) = -\frac{i\pi \rho_S [1 + \frac{\pi \rho_S \Gamma}{2} (1 - \frac{\Delta^2}{\epsilon^2})]}{\Upsilon} + \frac{i\pi \rho_S \frac{\Delta}{\epsilon} \tau_y \sigma_y}{\Upsilon}, \quad (26)$$

where $\Upsilon = 1 + \pi \rho_S \Gamma + \frac{\pi^2 \rho_S^2 \Gamma^2}{4} (1 - \frac{\Delta^2}{\epsilon^2})$ and $\Gamma = \Gamma_1 + \Gamma_2$. By inserting Eq. (26) into the Eqs. (18) and (19), one can obtain the tunneling coefficients

$$T_N(\epsilon) = \cos^2 \theta \Gamma_1 \Gamma_2 \left| -\frac{i\pi \rho_S [1 + \frac{\pi \rho_S \Gamma}{2} (1 - \frac{\Delta^2}{\epsilon^2})]}{\Upsilon} \right|^2, \quad (27)$$

$$T_{\text{CAR}}(\epsilon) = \sin^2 \frac{\theta}{2} \Gamma_1 \Gamma_2 \left| \frac{i\pi \rho_S \frac{\Delta}{\epsilon}}{\Upsilon} \right|^2. \quad (28)$$

The two scattering probabilities incorporate the relative spin rotation angle θ induced by the Rashba SOC in the helical edge states. This indicates that the manipulation of the edge state spin can be inferred from these probabilities, representing the main physical result of this paper.

III. DISCUSSIONS

The electron transmission probability (27) and CAR probability (28) between the two sets of edge states provide a direct measure of our control over the helical edge states, as illustrated in Fig. 1. We first examine the extreme cases where the Rashba SOC strengths $\lambda_{1,2}$ are 0 and infinity, corresponding to rotation angles $\theta_{1,2} = 0$ and $\theta_{1,2} = \pi/2$, respectively. In the absence of Rashba SOC, the probability of CAR is zero, and only electron transmission occurs at edge 2. This is because the incident electrons at edge 1 have spin-up polarization, while the outgoing states at edge 2 also possess spin-up polarization, resulting in a lack of spin-paired electrons to match the incident electrons and thereby preventing CAR. When Rashba SOC is present, it causes the spins of the two edges to rotate in opposite directions. As the Rashba SOC strength approaches infinity, the spin of the incident electron at edge 1 rotates clockwise by $\pi/2$ from spin-up to spin-right, while the spin of the outgoing state at edge 2 rotates counterclockwise from spin-up to spin-left, precisely opposite to the spin of the incident electron. This alignment enables the formation of Cooper pairs and facilitates CAR process. At this extreme, the outgoing spin is antiparallel to the incident spin, rendering the two states orthogonal and thus prohibiting electron transmission.

In general cases, Rashba SOC induces a clockwise rotation of the electron spin on edge 1 by an angle θ_1 , aligning the spin of the incident electron parallel to the direction \mathbf{m} . Conversely, the spin of the outgoing electron is oriented parallel to $-\mathbf{m}$. On edge 2, Rashba SOC causes the electron spin to rotate counterclockwise by an angle θ_2 , with the spin of the reflected electron parallel to the direction $-\mathbf{n}$. Thus, the electron transmission amplitude on edge 2 is proportional to $\langle \mathbf{m} | -\mathbf{n} \rangle = \cos \frac{\theta}{2}$. CAR necessitates the formation of Cooper pairs with spins oriented oppositely, so the outgoing hole's spin aligns with \mathbf{m} (corresponding to the vacancy of electron with spin state $|-\mathbf{m}\rangle$). The amplitude for this process is proportional to $\langle -\mathbf{m} | -\mathbf{n} \rangle = \langle \mathbf{m} | \mathbf{n} \rangle = \sin \frac{\theta}{2}$. Consequently, CAR provides a direct measure of the relative spin deflection angle $\theta = \theta_1 + \theta_2$ between the edge state spins at edges 1 and 2 under the influence of the Rashba SOC. Fig. 2 illustrates the variation of the CAR probability $T_{\text{CAR}}(\epsilon)$ and the electron transmission probability $T_{\text{N}}(\epsilon)$ as functions of incident energy for different angles θ . It is observed that both probabilities reach their maximum as the incident energy approaches the superconducting

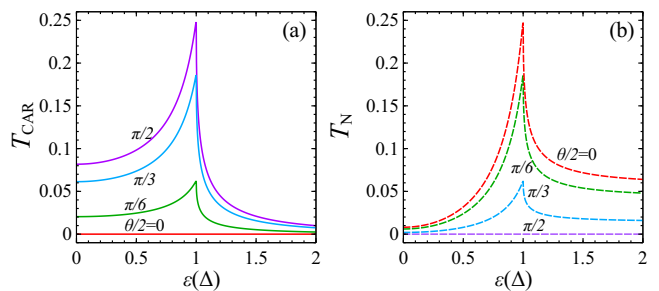


FIG. 2. (Color online) The CAR probability (a) and normal electron transmission probability (b) as functions of incident energy for different rotation angles θ . The linewidth functions are set to $\Gamma_1 = \Gamma_2 = 0.1$.

gap Δ , because the wave function decays more slowly in the superconductor when the energy is near the superconducting gap. Additionally, the CAR probability increases from zero to a finite value with increasing θ , while the probability of electron transmission decreases. These trends reflect the influence of Rashba SOC on the spin deflection of edge states.

The conductance of edge 2 is given by

$$G_2 = \frac{e^2}{h} (T_{\text{CAR}} - T_{\text{N}}). \quad (29)$$

Fig. 3 illustrates the dependence of conductance on the strength of Rashba SOC and incident energy. Notably, when $\lambda/v > 1$, a positive conductance is observed if the incident energy falls within the superconducting gap $\epsilon < \Delta$, indicating the dominance of CAR. When $\lambda/v < 1$, positive conductance appears only within low energy regions. Regardless of whether the conductance is positive, the control of the edge state spin will always be reflected through the change in conductance as the Rashba SOC varies.

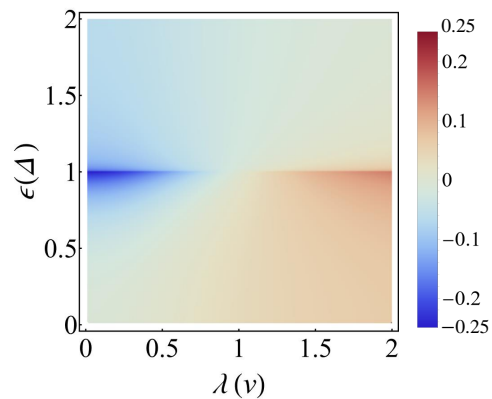


FIG. 3. (Color online) Differential conductance G_2 as functions of incident energy and Rashba SOC strength. The linewidth functions are set to $\Gamma_1 = \Gamma_2 = 0.1$.

Specifically, when the incident energy $\epsilon \rightarrow \Delta$, the transmission coefficient (27) and CAR coefficient (28) simplify to $T_N = \cos^2(\theta/2)\Gamma_1\Gamma_2/\Gamma^2$ and $T_A = \sin^2(\theta/2)\Gamma_1\Gamma_2/\Gamma^2$, respectively. Consequently, the conductance reduces to

$$G_2 = -\frac{e^2 \cos \theta \Gamma_1 \Gamma_2}{\hbar \Gamma^2}. \quad (30)$$

The conductance is directly related to the cosine of the relative rotation angle between the spins at the two edges, thereby clearly reflecting the influence of Rashba SOC on the modulation of edge state spin. The theoretical model encompassing helical edge states coupled with an s -wave superconductor heterostructure, the modulation of Rashba SOC through gate voltage, and the measurement of multi-terminal electron transport are all achievable with current experimental techniques. Thus, the theoretical scheme and results we present are directly applicable and realizable within existing experimental setups.

IV. SUMMARY

In this paper, we propose utilizing CAR to assess the efficiency of gate voltage control on edge state spin. We calculate the transport properties of a QSHIs-SOC

heterojunction using non-equilibrium Green's function method. Our results indicate that the CAR probability, electron transmission probability, and non-local conductance all incorporate the relative spin rotation angle θ , which arises from Rashba SOC in the helical edge states. Specifically, as the incident energy approaches the superconducting gap $\epsilon \rightarrow \Delta$, the differential conductance $G_2 \propto -\cos \theta$. Consequently, the influence of the Rashba SOC on edge state spin can be quantitatively evaluated through CAR, offering a practical approach for experimental validation.

V. ACKNOWLEDGMENTS

This work was supported by the National Natural Science Foundation of China under Grant No. 12074172 (W.C.), No. 1222406 (W.C.), and No. 12264019 (W.L.), the Natural Science Foundation of Jiangsu Province under Grant No. BK20233001 (W.C.), the Fundamental Research Funds for the Central Universities under No. 2024300415 (W.C.), the National Key Projects for Research and Development of China under No. 2022YFA120470 (W.C.), and the Jiangxi provincial Department of Science and Technology under Grant No. 20242BAB23005 (W.L.).

-
- [1] M. Z. Hasan and C. L. Kane, *Rev. Mod. Phys.* **82**, 3045 (2010).
 - [2] X.-L. Qi and S.-C. Zhang, *Rev. Mod. Phys.* **83**, 1057 (2011).
 - [3] B. A. Bernevig, T. L. Hughes, and S.-C. Zhang, *Science* **314**, 1757 (2006).
 - [4] M. König, S. Wiedmann, C. Bruene, A. Roth, H. Buhmann, L. W. Molenkamp, X.-L. Qi, and S.-C. Zhang, *Science* **318**, 766 (2007).
 - [5] A. Roth, C. Bruene, H. Buhmann, L. W. Molenkamp, J. Maciejko, X.-L. Qi, and S.-C. Zhang, *Science* **325**, 294 (2009).
 - [6] C. L. Kane and E. J. Mele, *Phys. Rev. Lett.* **95**, 226801 (2005).
 - [7] C. Wu, B. A. Bernevig, and S.-C. Zhang, *Phys. Rev. Lett.* **96**, 106401 (2006).
 - [8] X.-L. Qi, T. L. Hughes, and S.-C. Zhang, *Phys. Rev. B* **78**, 195424 (2008).
 - [9] J. Maciejko, E.-A. Kim, and X.-L. Qi, *Phys. Rev. B* **82**, 195409 (2010).
 - [10] V. Krueckl and K. Richter, *Phys. Rev. Lett.* **107**, 086803 (2011).
 - [11] F. Dolcini, *Phys. Rev. B* **83**, 165304 (2011).
 - [12] S. Modak, K. Sengupta, and D. Sen, *Phys. Rev. B* **86**, 205114 (2012).
 - [13] S. A. Wolf, D. D. Awschalom, R. A. Buhrman, J. M. Daughton, S. von Molnr, M. L. Roukes, A. Y. Chtchelkanova, and D. M. Treger, *Science* **294**, 1488 (2001).
 - [14] I. Zutic, J. Fabian, and S. Das Sarma, *Rev. Mod. Phys.* **76**, 323 (2004).
 - [15] S. S. P. Parkin, M. Hayashi, and M. Hayashi, *Science* **320**, 190 (2008).
 - [16] F. Meier, J. Levy, and D. Loss, *Phys. Rev. Lett.* **90**, 047901 (2003).
 - [17] M. Melzer, D. Makarov, A. Calvimontes, D. Karnausenko, S. Baunack, R. Kaltofen, R. Kaltofen, and O. G. Schmidt, *Nano Lett.* **11**, 2522 (2011).
 - [18] D. G. Rothe, R. W. Reinthaler, C.-X. Liu, L. W. Molenkamp, S. C. Zhang, and E. M. Hankiewicz, *New J. Phys.* **12**, 065012 (2010).
 - [19] A. Strom, H. Johannesson, and G. I. Japaridze, *Phys. Rev. Lett.* **104**, 256804 (2010).
 - [20] J. I. Vayrynen and T. Ojanen, *Phys. Rev. Lett.* **106**, 076803 (2011).
 - [21] P. Sternativo and F. Dolcini, *Phys. Rev. B* **89**, 035415 (2014).
 - [22] W. Chen, W.-Y. Deng, J.-M. Hou, D. N. Shi, L. Sheng, and D. Y. Xing, *Phys. Rev. Lett.* **117**, 076802 (2016).
 - [23] F. Ronetti, L. Vannucci, G. Dolcetto, M. Carrega, and M. Sasseti, *Phys. Rev. B* **93**, 165414 (2016).
 - [24] L. Ortiz, R. A. Molina, G. Platero, and A. M. Lunde, *Phys. Rev. B* **93**, 205431 (2016).
 - [25] J. H. Garcia, J. You, M. Garcia-Mota, P. Koval, P. Ordejon, R. Cuadrado, M. J. Verstraete, Z. Zanolli, and S. Roche, *Phys. Rev. B* **106**, L161410 (2022).
 - [26] E. I. Rashba, *Sov. Phys. Solid State* **2**, 1109 (1960).

- [27] J. M. Byers and M. E. Flatte, Phys. Rev. Lett. **74**, 306 (1995).
- [28] G. Deutscher and D. Feinberg, Appl. Phys. Lett. **76**, 487 (2000).